PHOTONICS Research

Watt-level and spectrally flat mid-infrared supercontinuum in fluoroindate fibers

Francis Théberge,[1,]* Nancy Bérubé,[1] Samuel Poulain,[2] Solenn Cozic,[2] Louis-Rafaël Robichaud,[3] Martin Bernier,[3] and Réal Vallée[3]

[1]*Defence R&D Canada, Valcartier Centre, Québec G3J 1X5, Canada*
[2]*Le Verre Fluoré, Campus KerLann, F-35170 Bruz, Brittany, France*
[3]*Center for Optics, Photonics and Lasers (COPL), Université Laval, Québec G1V 0A6, Canada*
Corresponding author: francis.theberge@drdc-rddc.gc.ca

We report on infrared supercontinuum (SC) generation in step-index fluoroindate-based fiber by using an all-fiber laser source. In comparison to widely used ZBLAN fibers for high-power mid-infrared (MIR) SC generation, fluoroindate fibers have multiphoton absorption edges at significantly longer wavelengths and can sustain similar intensities. Recent developments highlighted in the present study allowed the production of fluoroindate fibers with MIR background loss of 2 dB/km, which is similar to or even better than ZBLAN fibers. By using an all-fiber picosecond laser source based on an erbium amplifier followed by a thulium power amplifier, we demonstrate the generation of 1.0 W infrared SC spanning over 2.25 octaves from 1 μm to 5 μm. The generated MIR SC also exhibits high spectral flatness with a 6 dB spectral bandwidth from 1.91 μm to 4.77 μm and an average power two orders of magnitude greater than in previous demonstrations with a similar spectral distribution.   © 2018 Chinese Laser Press

OCIS codes: (060.2390) Fiber optics, infrared; (190.4370) Nonlinear optics, fibers; (320.6629) Supercontinuum generation.

https://doi.org/10.1364/PRJ.6.000609

1. INTRODUCTION

High brightness broadband sources in mid-infrared (MIR) atmospheric transmission windows have attracted a significant scientific interest in the past decade due to their wide range of potential uses in various fields, such as spectroscopy, metrology, as well as defense applications [1–3]. Supercontinuum (SC) sources using fluorozirconate-based fibers have reached watt level powers [4–9], some of which extended up to 4.7 μm by using short ZBLAN fibers [10], but usually the SC extensions are restricted to wavelengths below ~4.2 μm when using long ZBLAN fibers. A wavelength extension of the SC above 5 μm is possible when using fluoroindate glass fibers [11–13], allowing to completely cover the infrared atmospheric windows at 1.5–1.8 μm, 2.0–2.4 μm, and 3–5 μm for the aforementioned applications.

The intrinsic fiber loss due to the multiphonon absorption edge in fluorozirconate fibers is the main limitation on the long-wavelength side below ~4 μm of the generated SC. Emission beyond the multiphonon absorption edge can be achieved using small-core fibers of short lengths along with high pump intensities [14–17]. SC is also efficiently produced in chalcogenide (ChG) and tellurite fibers, given their very high nonlinear responses that are a few hundred times larger than in

fluoride fibers [18,19]. Demonstrations in ChG fibers yielded broader MIR supercontinuum; however, given that their zero-dispersion wavelength is usually above 4.5 μm, direct pumping with standard fiber lasers operating at wavelengths below 3 μm is not optimum. Extending SC beyond 4.5 μm in fluoride fibers is also important so as to be able to pump step-index ChG fibers and to further extend the SC through nonlinear propagation in cascaded fibers [20–22].

As shown in Table 1, there have been few demonstrations of infrared SC generation with fluoroindate fibers [6,11–13, 23–26] with some of them standing out due to their output powers or spectral bandwidths. Furthermore, SC flatness, which is important for many applications, has often been neglected. Previous works [6,24–26] reported that InF_3 fibers can sustain high average powers, while [13] showed that broadband and high spectral flatness MIR SC can be achieved by injecting picosecond laser pulses with a central wavelength around 2 μm.

In parallel to these demonstrations, a lot of effort has been made to produce higher purity fibers in order to decrease the detrimental effects of the MIR background loss on the SC broadening and its output power.

In this paper, we present, to the best of our knowledge, the first demonstration of watt-level, spectrally flat, and broadband

Table 1.   Characteristics of Fluoroindate-Fiber-Based SC Laser Sources[a]

Reference	Short Description	20 dB Spectral Range (μm)	Average Power (W)
[11]	70 fs OPA ($\lambda_c = 3.4$ μm) injected in 16 μm core InF$_3$ fiber	2.6–4.8	0.0001
[12]	Er-ZBLAN fiber amplifier injected in 13.5 μm core InF$_3$ fiber	2.5–5.3	0.008
[13]	70 ps OPO ($\lambda_c = 2.02$ μm) injected in 9 μm core InF$_3$ fiber	1.9–5.3	0.008
[23]	100 fs Tm-doped silica fiber laser injected in 7 μm core InF$_3$ fibers	1.25–4.2	0.25
[6]	100 ns Tm-doped silica fiber laser injected in 16.7 μm core InF$_3$ fibers	1.9–2.4	1.02
[24]	1 ns Er-doped and Tm-doped silica fiber injected in 9 μm core InF$_3$ fiber	1.87–3.9	1.4
[25]	35 ps Tm-doped silica fiber injected in 9 μm core InF$_3$ fiber	1.7–4.3	1.76
[26]	1 ns Er-doped silica fiber laser injected in 16.7 μm core InF$_3$ fibers	1.05–2.65	2.09

[a]OPA, optical parametric amplifier; λ_c, central laser wavelength; Er, erbium; OPO, optical parametric oscillator; Tm, thulium.

MIR SC in step-index InF$_3$ fiber pumped by an all-fiber laser source. An average output power of 1.0 W spanning from 1 μm to 5 μm is demonstrated with high-spectral flatness. The recent production of high-purity InF$_3$ fibers allowed these achievements, and these fibers exhibited an MIR background loss of 2 dB/km.

2. EXPERIMENTAL SETUP AND RESULTS

The fiber-laser source used is shown in Fig. 1(a) and is based on a 1.55 μm pigtailed semiconductor laser diode delivering 50 ps pulses at 1 MHz repetition rate, pre-amplified in an erbium (Er)-doped fiber and amplified in an erbium–ytterbium (Yb)-doped (10 μm core) double-clad silica fiber pumped at 980 nm. A broadband spectrum ranging from 1.2 μm to 2.5 μm with 1.9 W of average power was generated in the 1.5 m long undoped silica fiber (8 μm core diameter) from the combiner spliced at the output of the Er–Yb amplifier [see blue line in Fig. 1(b)].

The spectral components generated around 1.9 μm were preliminarily amplified in a thulium (Tm)-doped single-clad silica fiber and then spectrally filtered with a fiber isolator [see green line in Fig. 1(b)]. The signal around 1.9 μm was then further amplified in a 10 μm core diameter Tm-doped double-clad silica fiber having an effective absorption of 3 dB/m at the 791 nm pump wavelength. The unconverted part of the 1.55 μm pulse injected into the Tm amplifier was absorbed in the Tm-doped fiber and did not generate any significant output power. At low pump power, the amplified laser pulses have a narrower spectrum than at maximum pump power [see black and red lines in Fig. 1(b)]. The broadening of the amplified laser pulses is due to the Tm-doped fiber acting as a nonlinear and active medium. The 2.3 W output laser was butt-coupled using flat cleaves into an InF$_3$ fiber, as well as into a ZBLAN fiber for comparison, and both fluoride fibers were wound on a spool having a radius of 10 cm. The alignment of the butt-coupling was optimized by monitoring the SC output power and the spectral extension. Table 2 summarizes the main parameters for the fluoride fibers used in the experiment. The computation of ZBLAN dispersion was calculated with commercial software (Mode Solutions, Lumerical Inc. [27]) and was based on the Sellmeier equation with the coefficients from Ref. [28]. The index of refraction of the InF$_3$ fiber was measured from a bulk sample with an infrared ellipsometer. The theoretically estimated dispersion of the InF$_3$ fiber was confirmed for wavelengths between 2.3 μm and 2.5 μm by measuring the dispersion of an 81-cm long InF$_3$ fiber sample with a white-light interferometer.

The SC distribution was measured with an $f = 12.5$ cm monochromator purged with dry nitrogen and equipped with a 300 lines/mm diffraction grating to provide a spectral resolution of around 5 nm. The spectral fluence was measured with a PbSe detector for wavelengths between 1 μm and 4.8 μm and with a liquid nitrogen cooled HgCdTe detector from 2 μm to 13 μm. A set of long-pass filters was properly used in order to
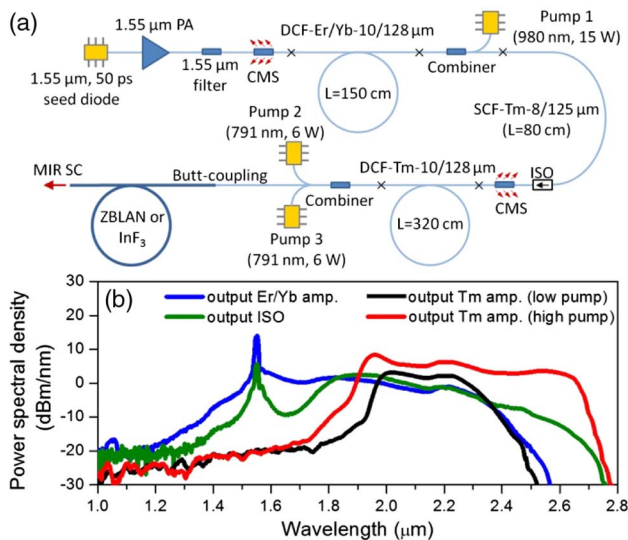
Fig. 1. (a) Experimental setup of the MIR SC fiber source. PA, pre-amplifier; CMS, cladding mode stripper; DCF, double-clad fiber; SCF, single-clad fiber; ISO, 2 μm optical isolator (Thorlabs, IO-K-2000); L, fiber length. (b) Spectral distribution of the Er/Yb amplifier (blue line), output of the fiber isolator (green line), and the Tm amplifier (black and red lines).

Table 2.   Fiber Parameters Summary[a]

| Parameter	ZBLAN	InF$_3$ Sample_A	InF$_3$ Sample_B
Core diameter (μm)	8.5	9.5	9
Clad diameter (μm)	125	100	100
ZDW (μm)	1.6	1.9	1.9
NA	0.23	0.3	0.3
Cutoff (μm)	2.4	3.7	3.4
Min. MIR loss (dB/m)	0.003	0.002	0.015
Manufacturer	LVF	LVF	LVF

[a]ZDW, zero dispersion wavelength; Min., minimum; LVF, Le Verre Fluoré.

block any higher diffraction orders of the grating from overlapping with the SC profile. The complete spectral response was calibrated with a blackbody radiation source (IR-508, Infrared Systems) for each combination of a detector and a long-pass filter.

At low powers from the Tm amplifier, the butt-coupling efficiencies between the Tm amplifier and the fluoride fibers were around 85%. At the maximum power from the Tm amplifier, the coupling efficiencies decreased to 56% for the ZBLAN fiber and to 60% for the two InF$_3$ fibers tested. The decrease of the coupling efficiency when increasing the pump power is due to the spectral broadening of the Tm-amplifier output and the increase of its mode field diameter (MFD) at longer wavelengths. At the output of the Tm-amplifier combiner [numerical aperture (NA) of 0.15, core diameter of 10 μm], the MFD increases from 11 μm to 14.5 μm for laser wavelengths from 2 μm to 2.7 μm, respectively, while the MFDs of ZBLAN and InF$_3$ fibers remain below 10 μm for this range of wavelengths. Therefore, as the pump power is increased, the output spectrum of the Tm amplifier broadens and the effective MFD increases, which reduce the butt-coupling efficiency with the following ZBLAN or InF$_3$ fibers. For the maximum output power of 2.3 W from the Tm amplifier, 1.3 W of pump power was coupled into InF$_3$ fibers and 1.27 W into the ZBLAN fiber. The corresponding SCs produced into the 20-m long fiber for the three fluoride fibers described in Table 2 are presented in Fig. 2(a). As a reference, the output spectrum of the Tm amplifier is also shown in Fig. 2(a). The corresponding attenuation, dispersion, and MFD spectra of InF$_3$ and ZBLAN fibers are shown in Figs. 2(b), 2(c), and 2(d), respectively.

The dynamics of the SC generation in optical fibers is well known. When a fiber is pumped with picosecond or nanosecond pulses in the anomalous dispersion region, modulation instability (MI) and self-phase modulation (SPM) are the main phenomena involved in the first step of SC generation. This MI leads to the temporal breakup of injected pulses into a distributed spectrum of many shorter subpulses, which then propagate through the fiber. Subsequently, each subpulse undergoes further spectral broadening through MI, SPM, as well as Raman soliton self-frequency shift [29].

It is interesting to note that for similar injected powers into those fluoride fibers, the MIR SC extension into ZBLAN fiber is limited to 4.3 μm with an output power of 0.75 W, while the SC generated in the low loss InF$_3$ fiber (sample A) extended up to 5 μm with 1 W of output power. When examining the MIR SC extension of ZBLAN and InF$_3$ (sample A) fibers in Fig. 2(a) along with their respective attenuations in Fig. 2(b) (blue and red lines), we clearly see that the multiphonon absorption edge was the main limitation to their long-wavelength extension. For all fluoride fibers used in this work, the bending loss at long wavelength is negligible. The lower NA of the ZBLAN fiber induces a larger MFD at longer wavelength [see Fig. 2(d)], which could also have contributed to reducing the spectral extension by decreasing the nonlinearity. Since the ZBLAN fiber and the first InF$_3$ fiber (sample A) exhibit a similar MIR background loss, the lower output power for the ZBLAN fiber is mainly due to the absorption of its MIR SC extending beyond
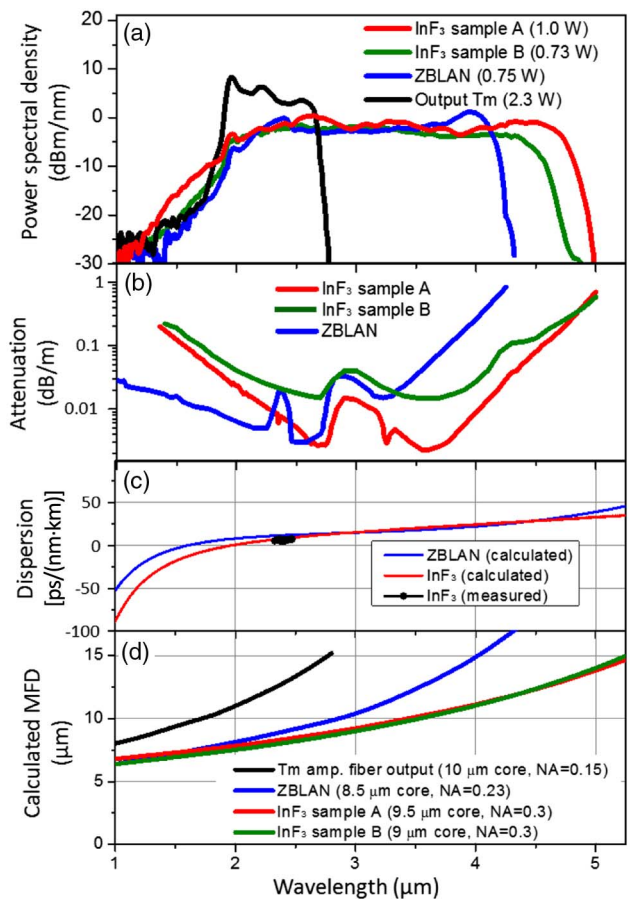
Fig. 2. (a) Spectral distribution of the Tm amplifier (black line) injected into fluoride fibers. The SCs from the 20-m ZBLAN and 20-m InF$_3$ fibers are shown with red, green, and blue lines, respectively. Corresponding SC output average powers are indicated in parentheses in the legend. (b) Measured attenuation and (c) calculated dispersion spectra of ZBLAN and InF$_3$ fibers. (d) Calculated mode field diameter (MFD) of fundamental modes in ZBLAN, InF$_3$, and silica fibers as a function of wavelength.

4 μm. As shown in Fig. 2(d), the MFD as a function of wavelength for both InF$_3$ fibers is very similar. However, in the case of the SC produced with the second InF$_3$ fiber (sample B), the output power and the MIR extension were lower because its MIR background loss was almost 10 times higher than for the first InF$_3$ fiber (sample A). Indirectly, the higher MIR background loss also reduced the fiber's MIR SC extension [see green line in Fig. 2(a)] since spectral broadening is driven by numerous nonlinear intensity-dependent processes. As a result of the MIR background loss, the laser pulse intensity decreased as it propagated along the fiber, reducing both the nonlinear effects and the MIR SC extension. Comparing both supercontinua from InF$_3$ fibers [green and red lines in Fig. 2(a)] clearly points to the importance of reducing the MIR background loss for SC generation in long fibers.

Figure 3(a) presents the SC distribution at the output of the InF$_3$ fiber (sample A) for increasing powers. Both the output average powers from the InF$_3$ fiber and the Tm amplifier (in parenthesis) are given in the legend of Fig. 3(a). As expected,
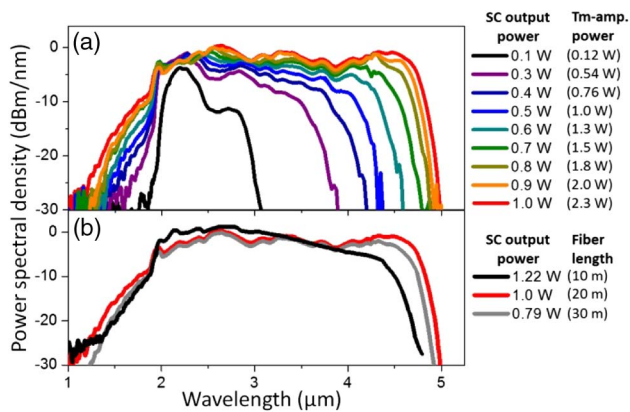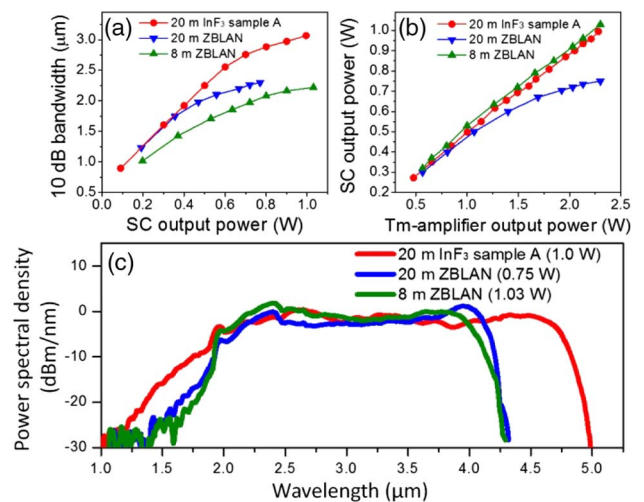
Fig. 3. (a) Spectral distribution at the output of the 20-m long InF$_3$ fiber (sample A) for different pump powers. (b) Spectral distribution at the output of the InF$_3$ fiber (sample A) for different fiber lengths. The laser power from the Tm amplifier was fixed to 2.3 W.

Fig. 4. (a) 10-dB spectral bandwidth as a function of the SC output power. (b) SC output power as a function of the Tm amplifier output power. (c) Spectral distribution at the output of fluoride fibers. The laser power from the Tm amplifier was fixed to 2.3 W for the three cases presented, and the SC output powers are indicated in parenthesis.

when the injected power into the InF$_3$ fiber increases, the MIR SC extends towards longer wavelengths, and the spectral flatness improves. Since the spectral broadening was asymmetric and accentuated towards longer wavelengths, it can be inferred that the Raman soliton self-frequency shift was a dominant process for the SC generation in these fibers with the pump source used.

For the first InF$_3$ fiber (sample A), the experimentally observed optimum length in terms of spectral broadening is 20 m. The use of a longer InF$_3$ fiber, e.g., 30 m long, did not increase the SC span, but reduced its output power by ∼210 mW due to the MIR background loss [see Fig. 3(b)]. On the other hand, the use of InF$_3$ fiber length shorter than 20 m increased the SC output power, but both the MIR SC extension and its spectral flatness were reduced. An example is shown in Fig. 3(b) for 10-m long InF$_3$ fiber (sample A) where the SC output power increased to 1.22 W. Similarly for ZBLAN, the optimum length in terms of the spectral broadening and the output power was experimentally observed for 8-m long fiber. This length is shorter than the optimum InF$_3$ fiber length in order to minimize the impact on the SC of the stronger absorption in ZBLAN fiber at longer wavelengths [see Fig. 2(b)].

For comparison purposes, Fig. 4(a) depicts the 10-dB spectral flatness at the output of the InF$_3$ (sample A, 20 m long) and ZBLAN fibers (8 m and 20 m long) as a function of their output powers. In both cases, the SC bandwidth increased at a slower rate when the SC MIR extension reached their respective multiphonon absorption edges. With 20 m long fibers, the SC bandwidth increase slowed down when output powers exceeded ∼700 mW in the case of InF$_3$ and ∼500 mW for ZBLAN. Using a shorter ZBLAN fiber (8 m long) allowed to reduce the detrimental effect of the long-wavelength absorption edge and to increase its output power up to 1.03 W [see Fig. 4(b)], a similar output power as for the 20-m long InF$_3$ fiber (sample A). However, optimizing the ZBLAN fiber length did not yield a broader SC output. As seen in Figs. 4(a) and 4(c), both lengths of ZBLAN fibers (8 m and 20 m) resulted in a similar MIR extension up to 4.3 μm, while the 20 m InF$_3$ fiber produced an SC up to 5 μm.

3. CONCLUSION

In summary, we demonstrated the first watt-level output power, spectrally flat and >2-octave SC generated in a step-index InF$_3$ fiber pumped by an all-fiber laser source. The longer multiphonon absorption edge in InF$_3$ fibers allowed to extend the SC to a longer MIR wavelength (up to 5 μm) as compared to ZBLAN fiber. The high output power and high-spectral flatness achieved here show the potential of InF$_3$-based fibers as reliable all-fiber SC sources covering important infrared atmospheric windows. In addition to their transmission, step-index InF$_3$ fibers exhibit favorable dispersion properties for SC generation when pumped within the Tm gain window, around 2 μm. Finally, for the scheme where fluoride fibers are concatenated with ChG fibers for further infrared extension of the SC [20–22], the use of InF$_3$ fiber instead of ZBLAN can lead to further extension of the MIR SC [30].

REFERENCES

1. S. Dupont, C. Petersen, J. Thøgersen, C. Agger, O. Bang, and S. R. Keiding, "IR microscopy utilizing intense supercontinuum light source," Opt. Express **20**, 4887–4892 (2012).
2. S. Lambert-Girard, M. Allard, M. Piché, and F. Babin, "Differential optical absorption spectroscopy lidar for mid-infrared gaseous measurements," Appl. Opt. **54**, 1647–1656 (2015).
3. M. N. Islam, M. J. Freeman, L. M. Peterson, K. Ke, A. Ifarraguerri, C. Bailey, F. Baxley, M. Wager, A. Absi, J. Leonard, H. Baker, and M. Rucci, "Field tests for round-trip imaging at a 1.4 km distance with change detection and ranging using a short-wave infrared supercontinuum laser," Appl. Opt. **55**, 1584–1602 (2016).

4. O. P. Kulkarni, V. V. Alexander, M. Kumar, M. J. Freeman, M. N. Islam, F. Terry, M. Neelakandan, and A. Chan, "Supercontinuum generation from ~1.9 to 4.5 μm in ZBLAN fiber with high average power generation beyond 3.8 μm using a thulium-doped fiber amplifier," J. Opt. Soc. Am. B **28**, 2486–2498 (2011).

5. J. Swiderski and M. Michalska, "High-power supercontinuum generation in a ZBLAN fiber with very efficient power distribution toward the mid-infrared," Opt. Lett. **39**, 910–913 (2014).

6. J. Swiderski, M. Michalska, C. Kieleck, M. Eichhorn, and G. Mazé, "High power supercontinuum generation in fluoride fibers pumped by 2 μm pulses," IEEE Photon. Technol. Lett. **26**, 150–153 (2014).

7. Z. Zheng, D. Ouyang, J. Zhao, M. Liu, S. Ruan, P. Yan, and J. Wang, "Scaling all-fiber mid-infrared supercontinuum up to 10 W-level based on thermal-spliced silica fiber and ZBLAN fiber," Photon. Res. **4**, 135–139 (2016).

8. K. Yin, B. Zhang, L. Yang, and J. Hou, "15.2 W spectrally flat all-fiber supercontinuum laser source with >1 W power beyond 3.8 μm," Opt. Lett. **42**, 2334–2337 (2017).

9. C. Kneis, B. Donelan, I. Manek-Hönninger, T. Robin, B. Cadier, M. Eichhorn, and C. Kieleck, "High-peak-power single-oscillator actively Q-switched mode-locked Tm³⁺-doped fiber laser and its application for high-average output power mid-IR supercontinuum generation in a ZBLAN fiber," Opt. Lett. **41**, 2545–2548 (2016).

10. P. M. Moselund, C. Petersen, L. Leick, J. S. Dam, P. Tidemand-Lichtenberg, and C. Pedersen, "Highly stable, all-fiber, high power ZBLAN supercontinuum source reaching 4.75 μm used for nanosecond mid-IR spectroscopy," in *Advanced Solid-State Lasers Congress* (2013), paper. JTh5A.9.

11. F. Théberge, J.-F. Daigle, D. Vincent, P. Mathieu, J. Fortin, B. E. Schmidt, N. Thiré, and F. Légaré, "Mid-infrared supercontinuum generation in fluoroindate fiber," Opt. Lett. **38**, 4683–4685 (2013).

12. J.-C. Gauthier, V. Fortin, J.-Y. Carrée, S. Poulain, M. Poulain, R. Vallée, and M. Bernier, "Mid-IR supercontinuum from 2.4 to 5.4 μm in a low-loss fluoroindate fiber," Opt. Lett. **41**, 1756–1759 (2016).

13. M. Michalska, J. Mikolajczyk, J. Woijas, and J. Swiderski, "Mid-infrared, super-flat, supercontinuum generation covering the 2–5 μm spectral band using a fluoroindate fibre pumped with picosecond pulses," Sci. Rep. **6**, 39138 (2016).

14. R. R. Gattass, L. B. Shaw, and J. S. Sanghera, "Microchip laser mid-infrared supercontinuum laser source based on an As₂Se₃ fiber," Opt. Lett. **39**, 3418–3420 (2014).

15. O. Mouawad, J. Picot-Clémente, F. Amrani, C. Strutynski, J. Fatome, B. Kibler, F. Désévédavy, G. Gadret, J.-C. Jules, D. Deng, Y. Ohishi, and F. Smektala, "Multioctave midinfrared supercontinuum generation in suspended-core chalcogenide fibers," Opt. Lett. **39**, 2684–2687 (2014).

16. C. R. Petersen, U. Møller, I. Kubat, B. Zhou, S. Dupont, J. Ramsay, T. Benson, S. Sujecki, N. Abdel-Moneim, Z. Tang, D. Furniss, A. Seddon, and O. Bang, "Mid-infrared supercontinuum covering the 1.4–13.3 μm molecular fingerprint region using ultra-high NA chalcogenide step-index fibre," Nat. Photonics **8**, 830–834 (2014).

17. T. Cheng, K. Nagasaka, T. H. Tuan, X. Xue, M. Matsumoto, H. Tezuka, T. Suzuki, and Y. Ohishi, "Mid-infrared supercontinuum generation spanning 2.0 to 15.1 μm in a chalcogenide step-index fiber," Opt. Lett. **41**, 2117–2120 (2016).

18. N. Tolstik, E. Sorokin, V. Kalashnikov, and I. Sorokina, "Soliton delivery of mid-IR femtosecond pulses with ZBLAN fiber," Opt. Mater. Express **2**, 1580–1587 (2012).

19. J. S. Sanghera, I. D. Aggarwal, L. B. Shaw, C. M. Florea, P. Pureza, V. Q. Nguyen, F. Kung, and I. D. Aggarwal, "Nonlinear properties of chalcogenide glass fibers," J. Optoelectron. Adv. Mater. **8**, 2148–2155 (2006).

20. L.-R. Robichaud, V. Fortin, J.-C. Gauthier, S. Châtigny, J.-F. Couillard, J.-L. Delarosbil, R. Vallée, and M. Bernier, "Compact 3–8 μm supercontinuum generation in a low-loss As₂Se₃ step-index fiber," Opt. Lett. **41**, 4605–4608 (2016).

21. C. R. Petersen, P. M. Moselund, C. Petersen, U. Møller, and O. Bang, "Spectral-temporal composition matters when cascading supercontinua into the mid-infrared," Opt. Express **24**, 749–758 (2016).

22. R. A. Martinez, G. Plant, K. Guo, B. Janiszewski, M. J. Freeman, R. L. Maynard, M. N. Islam, F. L. Terry, O. Alvarez, F. Chenard, R. Bedford, R. Gibson, and A. I. Ifarraguerri, "Mid-infrared supercontinuum generation from 1.6 to >11 μm using concatenated step-index fluoride and chalcogenide fibers," Opt. Lett. **43**, 296–299 (2018).

23. R. Salem, Z. Jiang, D. Liu, R. Pafchek, D. Gardner, P. Foy, M. Saad, D. Jenkins, A. Cable, and P. Fendel, "Mid-infrared supercontinuum generation spanning 1.8 octaves using step-index indium fluoride fiber pumped by a femtosecond fiber laser near 2 μm," Opt. Express **23**, 30592–30602 (2015).

24. M. Michalska, P. Grzes, P. Hlubina, and J. Swiderski, "Mid-infrared supercontinuum generation in a fluoroindate fiber with 1.4 W time-averaged power," Laser Phys. Lett. **15**, 045101 (2018).

25. S. Liang, L. Xu, Q. Fu, Y. Jung, D. P. Shepherd, D. J. Richardson, and S.-U. Alam, "295-kW peak power picosecond pulses from a thulium-doped-fiber MOPA and the generation of watt-level >2.5-octave supercontinuum extending up to 5 μm," Opt. Express **26**, 6490–6498 (2018).

26. J. Swiderski, F. Théberge, M. Michalska, P. Mathieu, and D. Vincent, "High average power supercontinuum generation in a fluoroindate fiber," Laser Phys. Lett. **11**, 015106 (2014).

27. www.lumerical.com.

28. L. Zhang, F. Gan, and P. Wang, "Evaluation of refractive-index and material dispersion in fluoride glasses," Appl. Opt. **33**, 50–56 (1994).

29. G. Genty, S. Coen, and J. M. Dudley, "Fiber supercontinuum sources (Invited)," J. Opt. Soc. Am. B **24**, 1771–1785 (2007).

30. F. Théberge, N. Bérubé, S. Poulain, S. Cozic, S. Châtigny, L.-R. Robichaud, L.-P. Pleau, M. Bernier, and R. Vallée, "Infrared supercontinuum generated in concatenated InF₃ and As₂Se₃ fibers," Opt. Express (submitted).